

Mechanics of the slaking of shales

Luis E. Vallejo*

*Department of Civil and Environmental Engineering, 949 Benedum Hall,
University of Pittsburgh, Pittsburgh, PA 15261, USA*

(Received October 31, 2010, Revised August 2, 2011, Accepted August 22, 2011)

Abstract. Waste fills resulting from coal mining should consist of large, free-draining sedimentary rocks fragments. The successful performance of these fills is related to the strength and durability of the individual rock fragments. When fills are made of shale fragments, some fragments will be durable and some will degrade into soil particles resulting from slaking and inter-particle point loads. The degraded material fills the voids between the intact fragments, and results in settlement. A laboratory program with point load and slake durability tests as well as thin section examination of sixty-eight shale samples from the Appalachian region of the United States revealed that pore micro-geometry has a major influence on degradation. Under saturated and unsaturated conditions, the shales absorb water, and the air in their pores is compressed, breaking the shales. This breakage was more pronounced in shales with smooth pore boundaries and having a diameter equal to or smaller than 0.060 mm. If the pore walls were rough, the air-pressure breaking mechanism was not effective. However, pore roughness (measured by the fractal dimension) had a detrimental effect on point load resistance. This study indicated that the optimum shales to resist both slaking as well as point loads are those that have pores with a fractal dimension equal to 1.425 and a diameter equal to or smaller than 0.06 mm.

Keywords: rock fills; shales; slaking; pores; capillarity; point load test; fractal; analysis.

1. Introduction

Waste fills resulting from coal mining should consist of large, free-draining sedimentary rocks fragments. In the Appalachian region of the United States, waste fills are constructed using the durable rock fill method. This method involves the dumping of rock fragments into valleys at their angle of repose (Welsh *et al.* 1987). The dumping could be in a single high lift or several smaller lifts. The lifts can range from between 20 meters to over 125 meters in thickness. These lifts are then graded to develop the final fill configuration. The material forming the rock fill is generally made of angular blast rock. The successful performance of these fills is directly related to the strength and durability of the individual rock fragments. When the fill is comprised of shales, it will be case that some of these shales are durable and do not break, whereas others will degrade into soil-size particles as a result of: (1) the compressive loads that act at the points of contact between fragments; and (2) the slaking that takes place when the shale fragments absorb water. The degradation of the shales into soil-size particles causes settlement of the waste fills during and after

*Professor, E-mail: vallejo@pitt.edu

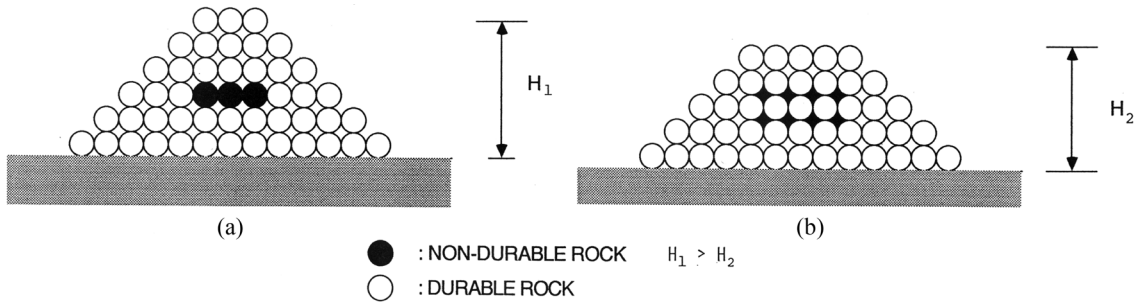


Fig. 1 Settlement of an embankment due to the slaking of non-durable shale particles

their construction (Sowers *et al.* 1965, Strohm 1978, Santi 1995, Oldecop and Alonso 2001, 2003). This kind of fill settlement can be explained with the use of Fig. 1. After completion, the waste fills are composed of durable and non-durable shale fragments (Fig. 1(a)). As slaking and crushing of the non-durable shale fragments commences, the slaked material moves from its original location and fills the voids located between the durable rock fragments. The movement of the slaked material into these voids is accomplished by gravity-induced point loads acting at the contacts between the fragments. These loads also cause the durable shale fragments to move into the space originally occupied by the non-durable shale fragments. The fragment replacement and void filling processes are the main causes of the settlement of waste fills (Fig. 1(b)).

The pore system forming part of rock fills are of two kinds. One is the inter-aggregate pore system, and the other is the intra-aggregate pore system (Fig. 2) (Koliji *et al.* 2006). Water can completely fill the inter-aggregate pore system (Fig. 2(a)); however it does not fill completely the intra-aggregate fill system because air pockets under pressure could be part of the micropores of

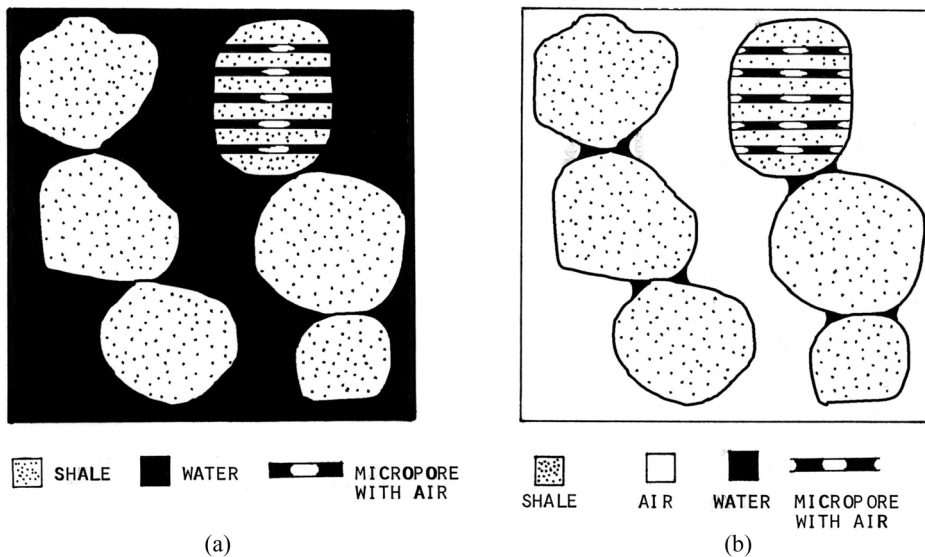


Fig. 2 (a) The inter-aggregate pore system in a granular assembly is saturated, the intra-aggregate pore system is unsaturated and (b) the inter-aggregate and the intra-aggregate pore systems are both unsaturated

the rock fragments. The air pockets form when water is sucked into the intra-aggregate pore system by capillary forces. Thus, if a rock fill is made of a rock and pore system as depicted in Fig. 2(a), the fill can be considered to be saturated if one considers only the inter-aggregate pore system, or unsaturated if one considers both the inter- and the intra-aggregate pore systems. However, when water partially fills both the inter- and intra-aggregate void systems (Fig. 2(b)), the fill is an unsaturated one.

In the present study, an assessment is made of the influence of the micro-geometry of the pore system in shales on their slaking when in contact with water as well as on their resistance to point loads. To conduct this assessment, sixty eight shale samples from surface coal mines from the Appalachia region of the United States were subjected to petrographic analyses that involved both thin section examination and X-ray diffraction analyses, as well as jar slake and point load tests.

2. Slake durability testing program

2.1 Shale samples

In order to understand the influence of pore wall geometry on the slaking of shales, and their resistance to point loads, sixty-eight shale samples were collected from near blasted high walls at surface mines in Kentucky, Tennessee, Virginia, and West Virginia. The samples were subjected in the laboratory to a combination of slake durability tests and thin section analysis. Image analysis of the photographs of the thin sections provided information about the pore geometry in the shale samples.

2.2 Durability and thin section analysis

In order to measure the durability of the shales when in contact with water, the jar slake test was used. In the jar slake test, air dried shale samples are immersed in water for a period of 24 hours. After this period, changes in the shale samples are evaluated using a ranking system (the jar slake index, I_j) which is based on the appearance of the samples after soaking. The ranking system was developed by Lutton (1977) and is shown in Table 1. In the system, the appearance of the sample is ranked from a value of 1 to a maximum value of 6 for the jar slake index, I_j .

The Lutton (1977) ranking system was applied to sixty-eight shale samples forming part of this study. Irregular-shaped dry samples weighing 100 grams were used for the jar slake test. Of the

Table 1 The slake ranking system by Lutton (1977)

The jar slake ranking, I_j	Behavior
1	Degrades to a pile of flakes or mud
2	Breaks rapidly and/or forms many chips
3	Breaks slowly and/or forms few chips
4	Breaks rapidly and/or develops several fractures
5	Breaks slowly and/or develops few fractures
6	No change

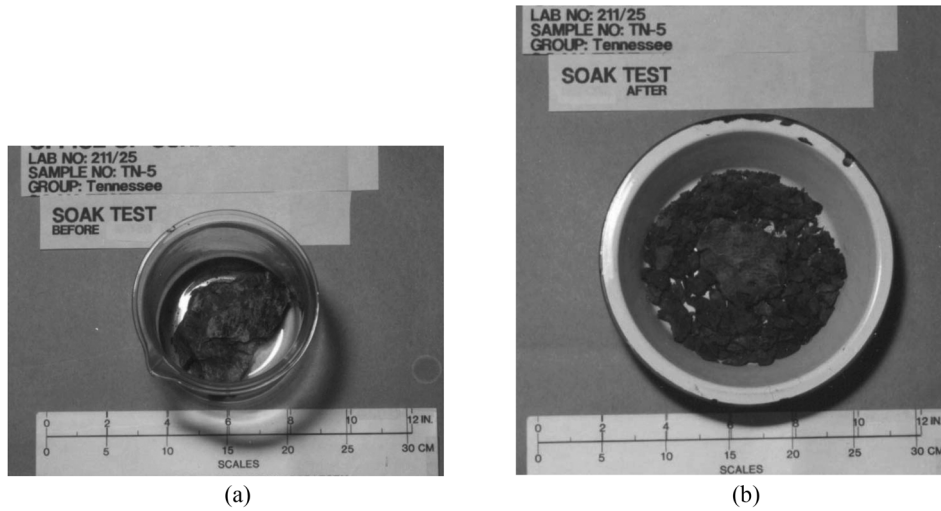


Fig. 3 (a) The TN-5 shale sample before soak test and (b) the TN-5 shale sample after soak test

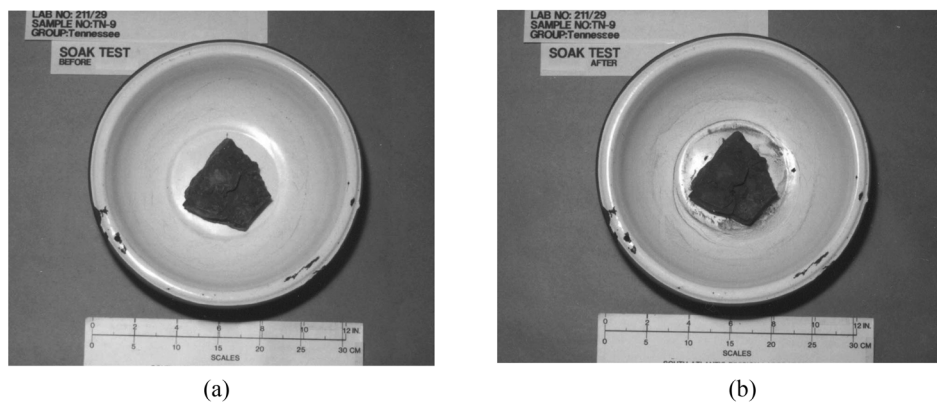


Fig. 4 (a) The TN-9 shale sample before soak test and (b) the TN-9 shale sample after soak test

sixty-eight shale samples tested, fourteen degraded into mud ($I_j = 1$), and fifty-four experienced little or no change ($I_j = 5$ or 6). Fig. 3 shows a sample from Tennessee (TN-5) with $I_j = 1$, and Fig. 4 shows a sample from Tennessee (TN-9) with an $I_j = 6$.

In addition to the jar slake test, the sixty-eight samples were subjected to X-ray diffraction analysis. The X-ray analysis indicated that the most prevalent clay mineral present in the shales was kaolinite (Table 2). The X-ray analysis also indicated that no expansive clay minerals were present in the samples. As a complement to the X-ray diffraction analysis, a thin section analysis of the shales was performed. This latter analysis involved the use of thin sections (30 mm in thickness) that were first examined optically with a polarizing microscope and then photographed.

2.3 Slaking mechanism

There are different mechanisms discussed in the geotechnical literature which explain the slaking

Table 2 X-ray diffraction analysis

Origin of shales and number	Kaolinite (%)	Quartz (%)	Mica (%)	Feldspar (%)	Other* (%)
Kentucky (30)	18	26	9	17	30
Tennessee (12)	6	42	26	5	21
Virginia (11)	8	30	37	6	19
West Virginia (15)	23	26	3	25	23

*Includes: Chlorite, Ankerite, Calcite, Siderites, and Opaques

of shales when immersed in water (Surendra *et al.* 1991, Yoshida and Hosokawa 2004). One slaking phenomenon is attributed to the compression of entrapped air in the pores of the shales when water enters them as a result of capillary suction (Moriwaki 1974). This entrapped air in the pores exerts tension on the solid skeleton, causing the material to fail in tension. According to Moriwaki (1974), pore-air compression is the predominant slaking mechanism in shales composed primarily of kaolinite. Since the sixty-eight shale samples tested in the jar slake test have kaolinite as the primary clay mineral in their structure (Table 2), pore-air compression is the primary mechanism causing their failure.

2.4 Pore air compression

The mechanism for pore-air compression that breaks the shales can be explained using Fig. 5. Fig. 5 shows a shale sample with a system of cylindrical intra-aggregate micropores that are assumed to be unconnected and run continuously through the sample (Fig. 5(a)). These micropores are assumed to resemble small cylindrical tubes inside the shale.

When the sample is in contact with water (Fig. 2), water will be pulled into the individual micropores as a result of capillary forces, and the air that originally filled the micropores will be subjected to compression (Fig. 5(b)). The system of forces acting at the interface between the air and the water in a micropore is presented in Fig. 5(c). At equilibrium conditions the following relationship applies

$$\pi d T_s - p(\pi d^2)/4 + u(\pi d^2)/4 = 0 \quad (1)$$

where d is the diameter of the cylindrical micropore, T_s is the surface tension of water acting on the meniscus, p is the air pressure, and u is the pore water pressure. The water pressure, u , is the resultant pressure from the water pressure at the two entrances of the cylinder and the water pressure at the meniscus (Fig. 5(b)) (Washburn 1921, Schmitt *et al.* 1994, Hilpert 2009).

From Eq. (1), the following relationship can be obtained

$$p = u + (4T_s)/d \quad (2)$$

An analysis of Eq. (2) indicates that the pore air pressure, p , in the portion of the micropore filled with air (Fig. 5(b)) increases as the diameter, d , of the cylindrical micropore decreases. Thus, the smaller the diameter of the micropore, the larger is the pore air pressure, p . Since pore-air compression is favored by small pore radii, slaking of the shales by air compression will be more pronounced in those shales containing micropores with small diameters. In addition, small diameter

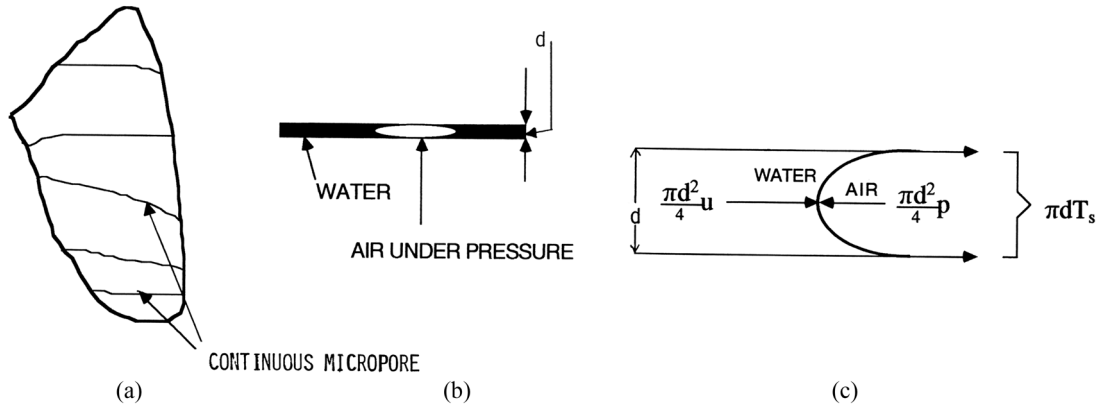


Fig. 5 (a) Shale sample with micropores, (b) micropore with water and air pressures and (c) air and water forces at the air-water interface in a micropore

micropores more readily confine the air pressure developed during the suction process. That is, the diffusion of the air pressure will decrease with a decrease in surface area (which is a function of the diameter of the micropore) of the pore that is in contact with the air. Thus, the diameter of the micropores in shales has a marked influence on their slaking with water.

2.5 Pore diameter of the micropores

The pore diameters of the sixty-eight shale samples were obtained from thin sections of the shales. The thin sections were $30 \mu\text{m}$ in thickness and had the shape of a square with a length equal to 25 mm. The preparation of the thin sections (cutting and grinding) followed the procedure outlined by Humphries (1992). Photographs of the thin sections were made using a polarizing microscope. From the photographs, the cross sectional areas and the perimeters of the pores in the shales were obtained. Using a standard digitizing software (AUTOCAD 2007), each individual was outlined by visual estimation of its boundary and modeled as a polygon in the program. The area and perimeter of each individual polygon representing the pore system in each thin section analyzed were determined by the software and recorded for use in the fractal analysis. Figs. 6 and 7 show the typical results of the process outlined above for the case of shales TN-5 and TN-9.

The average diameter of the pores in the TN-5 sample was equal to 0.053 mm. The diameter of each pore was equal to the diameter of an equivalent circle with area equal to that of the rough pore. The digitizing software used this approach for calculating the average diameter of the pores. Even though the pores in the shales are not circles, the equivalent circle approach has been used before by Means and Parcher (1963), Terzaghi and Peck (1968), and Bear (1972) to represent the pore structure in soils and rocks as seen in the thin sections. Also, this circular representation allows the use of Eq. (2). The average diameter of the rough pores in the TN-9 sample was equal to 0.107 mm.

The jar slake index, I_j , for TN-5 was equal to 1. The jar slake index, I_j , for TN-9 was equal to 6. The fourteen samples that degraded into soils had average pore diameters that were equal to or smaller than 0.06 mm. Fifty-four samples did not slake. Most of these samples had average pore diameters that were greater than 0.06 mm. However, eight of the fifty-four samples that did not

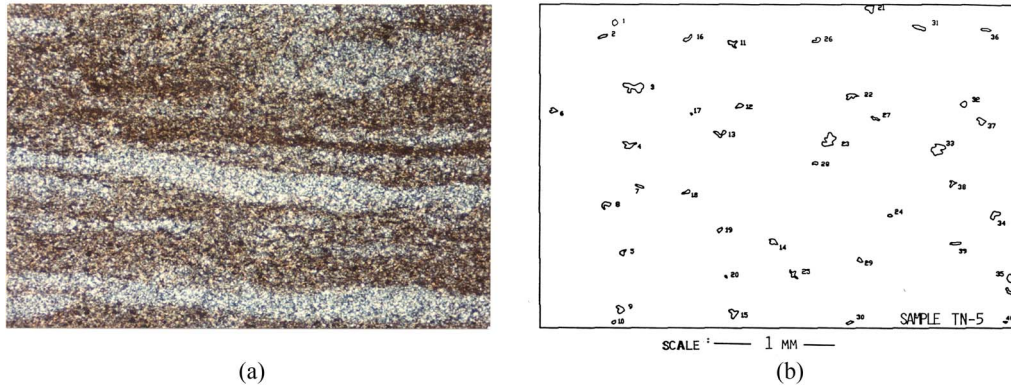


Fig. 6 (a) Micro-photograph of TN-5 shale sample and (b) pore geometry obtained from micro-photograph

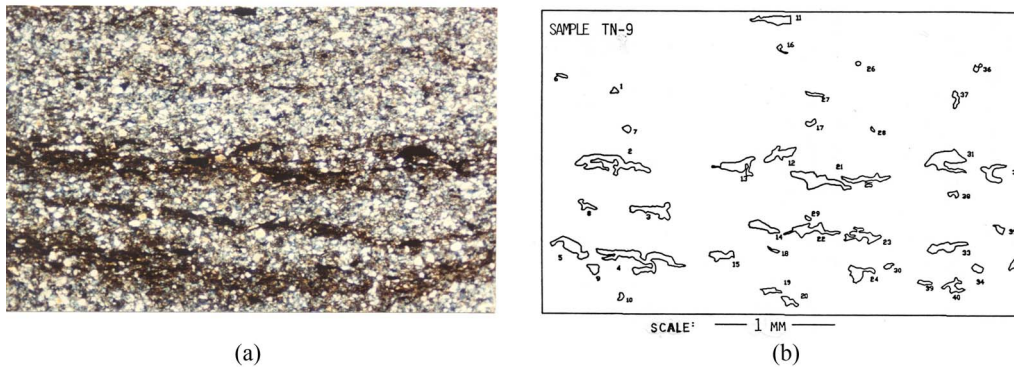


Fig. 7 (a) Micro-photograph of TN-9 shale sample and (b) pore geometry obtained from micro-photograph

slake had average pore diameters that were smaller than 0.06 mm. An explanation for why these eight samples failed to follow the smaller than 0.06 mm pore diameter rule follows next. This explanation uses fractal theory.

2.6 Measurement of pore wall roughness

The roughness of the pore boundaries was evaluated using fractal theory. Fractal theory makes use of a number called the fractal dimension, D , to evaluate the degree of irregularity of objects in nature (Mandelbrot 1977). In this study, the fractal dimension was used to measure the average degree of roughness of the pore boundaries of the sixty-eight shale samples. These pore boundaries are assumed to represent those obtained when the thin slice cut the pores in a direction normal to their long axis (Fig. 5). The fractal dimension of the pore boundaries was calculated using the area-perimeter method (Korvin 1992, Hyslip and Vallejo 1997). The fractal dimension, D , is obtained from the slope, m , of the best fit line that connects the values of the area and perimeter for each of the pores in a shale sample (Figs. 6 and 7). Fig. 8 shows this plot for the samples TN-5 and TN-9. Once the slope, m , is obtained, the dimension is calculated from the ratio between 2 and m (that is, $D = 2/m$). The fractal dimension, D , measures the average roughness of all the pore boundaries in

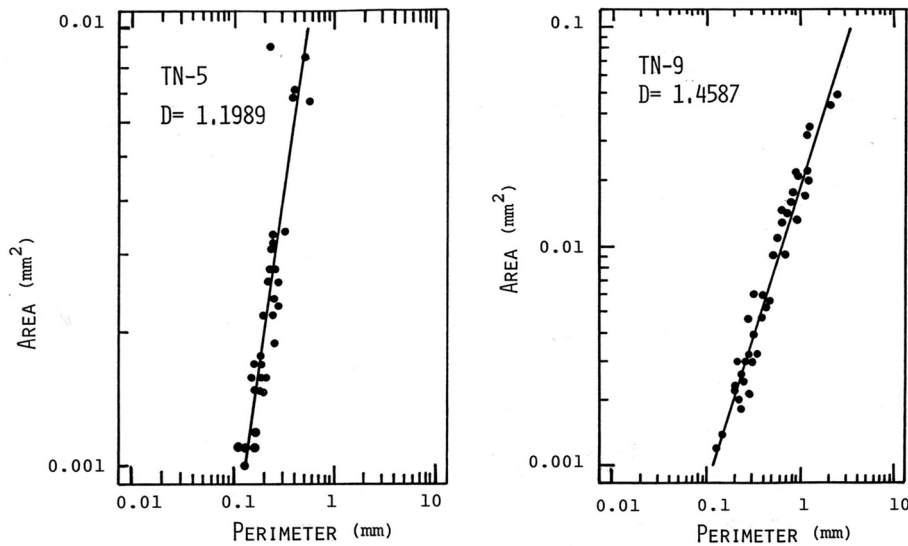


Fig. 8 Area-perimeter method to obtain the fractal dimension, D , of the pores in samples TN-5 and TN-9

the shale samples. The higher the value of D , the rougher are the pore boundaries in the shales. The fractal dimension, D , for all the pore boundaries of sample TN-5 (Fig. 6) was equal to 1.1989 (Fig. 8); D for sample TN-9 was equal to 1.4587 (Fig. 8). If one wants to obtain the fractal dimension of one pore, the area-perimeter method cannot be used. To do this calculation, one can use the ruler method (Hyslip and Vallejo 1997).

2.7 Pore diameter and degree of slaking

As previously mentioned, from the jar slake tests on the sixty-eight shale samples, fourteen slaked ($I_j = 1$). These slaked samples had average pore diameters equal to or smaller than 0.06 mm. Of the fifty-four samples that did not slake ($I_j = 5$ or 6), eight samples had diameters smaller than 0.06 mm. Thus, the size of the pore alone does not seem to explain completely why the shales slake as a result of pore air-compression as stated by Eq. (2).

2.8 The influence of pore wall roughness on the slaking of shales

Even though the size of the pores in shales is a good indicator for their slaking susceptibility, it was not a parameter that indicated without a doubt their slaking behavior. Table 3 shows the results of the jar slake tests and the fractal analysis on the eight samples that did not slake even though their average pore diameter was smaller than 0.06 mm. The fractal analysis for these shales indicated that their pore walls were very rough (Table 3 and Fig. 9). The high degree of roughness of the pore walls is reflected in their high values of the fractal dimension. An explanation for the lack of slaking for the shales of Table 3 that have small but rough pores seems to rest on the degree of roughness of these pores.

According to Ransohoff and Radke (1988), when a capillary tube with either a square or irregular cross section as shown in Fig. 10(a) is immersed in water, the water does not advance in the

Table 3 Properties of the eight shale samples with small pore diameters ($d < 0.06$ mm) that did not slake

Sample	Diameter (mm)	Jar slake index, I_j	Fractal dimension D	Water content, w_a (%)	Point load index I_{pa} (MPa)	Water content w_s (%)	Point load index, I_{ps} (MPa)
TN-7	0.056	6	1.7767	0.7	4.11	2.0	0.3
KY-32	0.055	5	1.6020	0.65	4.4	2.9	0.31
WV-8	0.052	5	1.5473	0.60	5.3	2.7	0.5
KY-19	0.052	6	1.4907	0.7	5.9	2.3	0.42
KY-22	0.051	6	1.4900	0.7	6.0	3.0	1.39
TN-17	0.056	6	1.4707	0.7	6.14	1.3	1.4
WV -14	0.051	5	1.4406	0.6	6.20	1.4	1.8
TN-16	0.050	6	1.4246	0.6	6.7	1.5	3.6

w_a = water content of the air dried samples; w_s = water content of the immersed in water samples; I_{pa} = point load strength of air dried samples; I_{ps} = point load strength of immersed in water samples

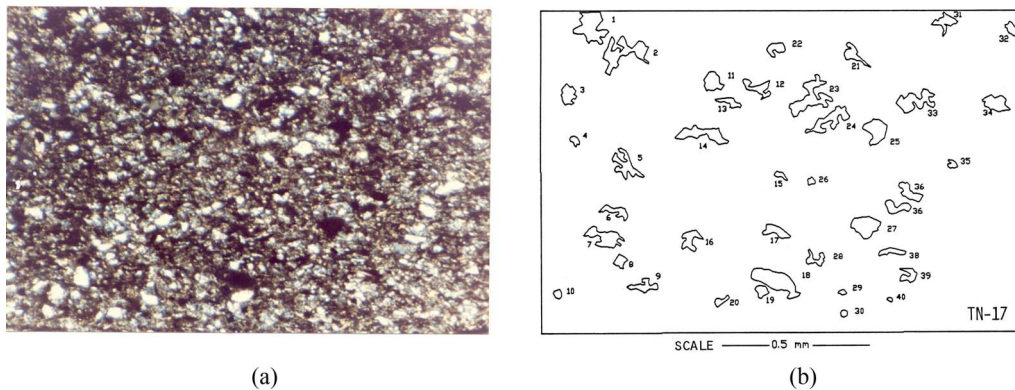


Fig. 9 (a) Micro-photograph of TN-17 shale sample and (b) rough pore geometry obtained from micro-photograph

capillary tube following the whole cross sectional area, but advances in the tube following its corners and crannies. This partial filling of the tube cross sectional area will prevent the development of air pressure that is necessary to cause the slaking of the shales. Fig. 10(b) shows how water will advance in a rough pore such as that shown in Figs. 7 and 9. The water at the extreme portions of the micropore will cover its whole cross sectional area. However, after moving a short distance from the ends of the micropore, the water will follow the corners and crannies of the pore walls (Fig. 9). This movement of the water through the corners and crannies of the pore walls will prevent the development of the air pressure that is required to cause the breakage of the shale (Fig. 5(b)). Thus, the roughness of the boundaries of the pores (measured by the fractal dimension) has a significant influence on the slaking of the shales and needs to be considered in any evaluation of the durability of shales in water, as well as on their point load strength.

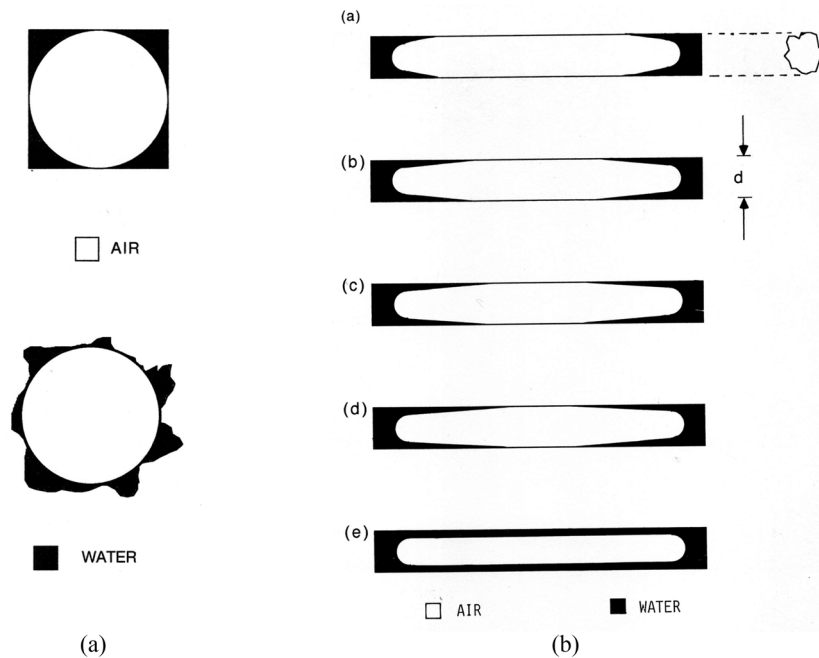


Fig. 10 (a) Capillary water flow in a micropore with rough pore walls and (b) the lack of air pressures in a micropore with rough pore walls

3. Point load testing program

Gravity loads are resisted by rock fragments forming part of a rock fill through force chains that the fragments develop when they interact at their points of contact (Cundall and Strack 1979). The effect of these force chains on the fill's fragments can be evaluated by the point load test.

Point load testing involves the loading of a rock lump of an average diameter, d_p , between two cone-shaped platens. The load, P , necessary for breaking the rock is measured. This load value, divided by the square of the diameter, d_p , provides the point load strength, I_p . The reported I_p values are the mean values after testing twenty lumps with the respective pore diameter and degree of roughness. According to Oakland and Lovell (1972), twenty lumps is the minimum number needed to obtain a statistically representative value of I_p for the rock fragments.

3.1 The effect of pore diameter on resistance to point loads

In order to determine if the pore diameter had an influence on the crushing by point loads of shale fragments, point load strength values were correlated with the values of the average diameter of the pores in the shales. The samples tested came from a site in Kentucky. Since the water content has a large influence on the point load strength of rocks (Broch and Franklin 1972), samples with very similar water contents were chosen for the correlations. Also, according to the same authors, the drier the rock samples tested in the point load apparatus are, the more reliable are the point load strength values. This is because the saturation of the samples could induce plastic yielding of the rock fabric beneath the point loads, affecting the results of the test. For this reason, the correlations

Table 4 Samples used to correlate point load strength and pore diameter

Sample	Pore diameter (mm)	Water content, w_a (%)	Point load index, I_{pa} (MPa)	Jar slake index, I_j
KY-B-6	0.0543	0.31	6.20	6
KY-A-23	0.0554	0.32	5.80	6
KY-16	0.081	0.30	3.28	6
KY-A-18	0.18	0.36	2.80	6

w_a = water content of the air dried samples; I_{pa} = point load strength of air dried samples

between point load strength (I_p) in the samples and their respective average pore diameter were done for the water contents that the samples acquired after air drying them for a period of 5 days. The air temperature during the drying period was equal to 20 degrees centigrade. The properties and the pore diameter for the samples tested are shown in Table 4.

An analysis of Table 4 indicates that the size of the pores influences the point load strength of the rock samples. Samples with smaller pore diameters had a higher value of point load strength.

3.2 The effect of pore wall roughness on resistance to point loads

The non-slaking shales whose properties are indicated in Table 3 were also subjected to point load tests. This was done to evaluate the effect of pore wall roughness on the point load strength. Table 3 shows the results of the point load tests on unsaturated samples having two different water contents, similar pore diameters and different fractal dimension values. The samples with the smaller water contents represented samples that were subjected to air drying for a period of 5 days. The air temperature during air drying was equal to 20 degrees centigrade. The higher water content samples were obtained by immersing them in water for a period of five days.

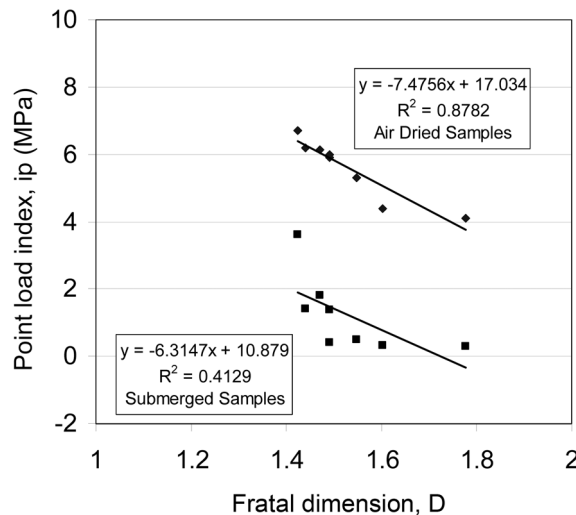


Fig. 11 Relationship between load point index, I_p , and the pores' fractal dimension, D , for the shale samples of Table 3

Fig. 11 shows a plot of the point load index, I_p , versus the fractal dimension value, D , of the pore walls forming part of the non-slaking shales of Table 3. Fig. 11 and Table 3 shows that the roughness of the pores has a detrimental effect on the point load strength. Fig. 11 shows that for the cases of the air dried and immersed samples, the point load strength decreased with an increase in fractal dimension values. The shale sample TN-16 was the non-slaking shale (average pore diameter $d = 0.05$ mm) that had the highest point load strength ($I_{pa} = 6.7$ MPa, and $I_{ps} = 3.6$ MPa) for the two water contents used in the point load tests. Rock fragments with these levels of point load resistance have been found by Indraratna (1994) to function successfully in rock fills. This study has established that the optimum shales to resist both slaking as well as point loads are those that have pores with a fractal dimension equal to 1.425 and a diameter equal to or smaller than 0.06 mm. An example of this optimum shale is TN-16 (Fig. 11 and Table 3).

4. Conclusions

The durability and strength of shales forming part of unsaturated and saturated rock fills were analyzed using a combination of slake durability and point load tests, thin section photographs and fractal theory. From these analyses, the following conclusions can be made:

- (1) The slaking of the shales studied was the result of pore air compression.
- (2) The slaking by pore air compression was directly related to the average pore diameter and the roughness of the pore boundaries. The smaller the diameter and the smoother the boundaries of the pores, the more pronounced was the slaking of the shales by air compression.
- (3) The roughness of the pore boundaries in the shales was determined using the fractal dimension concept from fractal theory. The larger the fractal dimension, the rougher were the boundaries of the pores.
- (4) Regardless of the diameter of the pores, shales with very rough pores did not slake as a result of pore air compression. These rough pores moved the capillary water through their corners and crannies. Thus, the water did not move through the whole cross sectional area of the rough pores. This type of water movement prevented the development of pore air compression that is needed for the breaking of the shales.
- (5) Pore diameter in the shales influenced their resistance to point loads. It was determined that the smaller the pore diameter was in the shales, the larger was their resistance to point loads.
- (6) Pore wall roughness also influenced their resistance to point loads. It was determined that the rougher the pore walls was in the shales, the smaller was their resistance to point loads.
- (7) From the shales studied, it was determined that the optimum shale to resist successfully both slaking as well as point loads is the one that has pores with a fractal dimension equal to 1.425 and an average diameter equal to or smaller than 0.06 mm.

References

- AUTOCAD (2007), *Autodesk, Inc.*, New York.
 Bear, J. (1972), *Dynamics of fluids in porous media*, Dover Publications, Inc., New York.
 Broch, E. and Franklin, J.A. (1972), "The point load strength", *Int. J. Rock Mech. Min. Sci.*, **9**, 669-697.
 Cundall, P.A. and Strack, O.D.L. (1979), "A discrete numerical model for granular assemblies", *Geotechnique*,

- 29(1), 47-65.
- Korvin, G. (1992), *Fractal models in the earth sciences*, Elsevier, Amsterdam.
- Hilpert, M. (2009), "Effects of dynamic contact angle on liquid infiltration into horizontal capillary tubes: semi-analytical solutions", *J. Colloid Interf. Sci.*, **337**, 131-137.
- Humphries, D.W. (1992), *The preparation of thin sections of rocks, minerals and ceramics*, Royal Microscopical Society Microscopic Handbooks, Oxford Science Publications, Oxford.
- Hyslip, J.P. and Vallejo, L.E. (1997), "Fractal analysis of the roughness and size distribution of granular materials", *Eng. Geology*, **48**(3-4), 231-244.
- Indraratna, B. (1994), "The effect of normal stress-friction angle relationship on the stability analysis of a rockfill dam", *Geotech. Geol. Eng.*, **12**, 113-121.
- Koliji, A., Laloui, L., Cusinier, O. and Vulliet, L. (2006), "Suction induced effects on the fabric of a structured soil", *Transport Porous Med.*, **64**, 261-278.
- Lutton, R.J. (1977), *Design and construction of compacted shale embankments: slaking indices for design*, Report FHWA-RD-1, Federal Highway Administration, Washington, D.C.
- Mandelbrot, B.B. (1977), *Fractals: form, chance and dimension*, W.H. Freeman, San Francisco.
- Means, R.E. and Parcher, J.V. (1963), *Physical properties of soils*, Charles E. Merrill Books Inc. Columbus, Ohio.
- Moriwaki, Y. (1974), *Causes of slaking of argillaceous materials*, Ph.D. Dissertation, Dept. of Civil Engineering, University of California at Berkeley.
- Oakland, M.W. and Lovell, C.W. (1982), "Classification and other standard tests of shale embankments", *Joint Highway Research Project Report 82-4*, Purdue University, West Lafayette, Indiana, 171 p.
- Oldecop, L.A. and Alonso, E.E. (2001), "A model for rockfill compressibility", *Geotechnique*, **51**(2), 127-139.
- Oldecop, L.A. and Alonso, E.E. (2003), "Suction effects on rockfill compressibility", *Geotechnique*, **53**(2), 289-292.
- Ransoff, T.C. and Radke, C.J. (1988), "Laminar flow of a wetting liquid along corners of predominantly gas occupied non circular pores", *J. Colloid Interf. Sci.*, **121**(2), 391-401.
- Santi, P.M. (1995), "Assessing the strength and durability properties of shales", In: *Landslides Under Static and Dynamic Conditions-Analysis, Monitoring, and Mitigation*, *Geotechnical Special Publication*, No. 52, American Society of Civil Engineers, Keefer, D.K., and Ho, C.L., Editors, pp.37-55.
- Schmitt, L., Forsans, T. and Santarelli, F.J. (1994), "Shale testing and capillary phenomena", *Int. J. Rock Mech. Min. Sci.*, **31**(5), 411-427.
- Sowers, G.F., Williams, R.C. and Wallace, T.C. (1965), "Compressibility of broken rock and the settlement of rock fills", *Proceedings of the 6th Int. Conf. on Soil Mechanics and Foundation Eng., Paris*, **II**, 561-565.
- Strohm, W.E. (1978), "Design and construction of compacted shale embankments: field and laboratory investigations", *Report FHWA-RD-78-140*, Federal Highway Administration, Washington D.C., 146 p.
- Surendra, M., Lovell, C.W. and Wood, L.E. (1981), "Laboratory studies of the stabilization of non-durable shales", *Transport. Res. Record*, **79**, 33-40.
- Terzaghi, K. and Peck, R.B. (1968), *Soil mechanics in engineering practice*, John Wiley and Sons, New York.
- Washburn, E.W. (1921), "The dynamics of capillary flow", *Phys. Rev.*, **17**(3), 273-283.
- Welsh, R.A., Vallejo, L.E. and Robinson, M.K. (1987), "Evaluation of durability testing techniques for rock underdrain material used in Appalachian surface coal mining valley fills", *Proceedings of the Int. Symposium on Flow Trough Rock Drains*, Cranbrook, Canada, **I**, 83-93.
- Yoshida, N. and Hosokawa, K. (2004), *J. Geotech. Environ. Eng.*, **130**(5), 519-525.